CHEMISTRY
A EUROPEAN JOURNAL

DOI: 10.1002/chem.201003255

Lanthanide-Containing Photoluminescent Materials: From Hybrid Hydrogel to Inorganic Nanotubes

Yan Qiao, Yiyang Lin, Shaofei Zhang, and Jianbin Huang*[a]

Abstract: Functional photoluminescent materials are emerging as a fascinating subject with versatile applicability. In this work, luminescent organic–inorganic hybrid hydrogels are facilely designed through supramolecular self-assembly of sodium cholate, and lanthanide ions such as Eu^{3+}, Tb^{3+}, and Eu^{3+}/Tb^{3+}. Fluorescence microscopy and TEM visualization demonstrates the existence of spontaneously self-assembled nanofibers and 3D networks in hybrid hydrogel. Photoluminescence enhancement of lanthanide ions is realized through coordination with cholate and co-assembly into 1D nanofibers, which can successfully shield the Eu^{3+} from being quenched by water. The photoluminescence emission intensity of a hybrid hydrogel exhibits strong dependence on europium/cholate molar ratio, with maximum emission appearing at a stoichiometry of 1:3. Furthermore, the emission color of a lanthanide–cholate hydrogel can be tuned by utilizing different lanthanide ions or co-doping ions. Moreover, photoluminescent lanthanide oxysulfide inorganic nanotubes are synthesized by means of a self-templating approach based on lanthanide–cholate supramolecular hydrogels. To the best of our knowledge, this is the first time that the lanthanide oxysulfide inorganic nanotubes are prepared in solution under mild conditions.

Keywords: hydrogel · lanthanide · nanotubes · photoluminescence · self-assembly

Introduction

The photoluminescence properties of trivalent lanthanide ions have aroused tremendous interest for decades owing to their broad applicability in medical diagnostics, cell imaging, and functional nanomaterials.[1] The attractive features of lanthanide ions as luminescent materials include their line-like emission, high quantum yield, long luminescence lifetime (μs–ms range), high photochemical stability, and low long-term toxicity.[2] Up to now, most of the studies on lanthanide ions have been limited to either molecular lanthanide compounds (for instance, the β-diketonate complexes) or inorganic compounds (lanthanide phosphors).[3] Recently lanthanide-containing organic–inorganic hybrid materials, which combine the characteristics of organic and inorganic components at the nanoscale, are emerging as a hot topic.[4] The study of luminescent lanthanide hybrid materials is not only of fundamental interest; their advantageous versatility as optical materials characterized by good mechanical properties, ease of shaping and patterning, excellent optical quality, as well as a relatively facile synthesis makes them broadly applicable.

Supramolecular hydrogels represent a type of new soft material that is formed predominantly by preferential 1D self-assembly of organic gelators.[5] The hydrogel is usually composed of elongated fibrous aggregates with nanometer-scale diameters and micrometer-scale lengths that cross-link into 3D networks to entrap the solvent. Owing to their intriguing properties, supramolecular hydrogels formed by low-molecular weight gelators find applications in drug delivery, wound healing, template-directed synthesis, and as scaffolds for tissue engineering.[6] It has been realized that the incorporation of lanthanide ions into supramolecular hydrogel systems can generate novel functional materials with the combined advantages of photoluminescent performance and that may be applied in the fields of optical fibers, devices and sensors.[7] Furthermore, lanthanide-containing hydrogels are potential soft templates for synthesis of 1D luminescent inorganic nanomaterials under mild conditions. To date, the study of lanthanide-containing hydrogels has been seldom reported.[8] Žinić and De Cola have disclosed the development of reversible luminescent gels containing a carboxylate-based aliphatic gelator and an Eu^{III} hemicaged complex. Binnemans and Kato reported liquid-crystalline (LC) physical gels consisting of 4-pentyl-4′-cyanobiphenyl with amino acid-based gelators by doping a red-emitting molecular Eu^{III} complex. Quignard has described a photoluminescent hybrid hydrogel that contains alginate and lanthanide ions. Also, Rowan reported luminescent gel-like metallo-supramolecular polymers prepared from a monomer unit, which consists of a 2,6-bis-(benzimidazolyl)-4-hydroxypyri-

[a] Y. Qiao, Y. Lin, S. Zhang, Prof. Dr. J. Huang
Beijing National Laboratory for Molecular Sciences (BNLMS)
State Key Laboratory for Structural Chemistry of Unstable and Stable Species
College of Chemistry and Molecular Engineering
Peking University, Beijing 100871 (P. R. of China)
Fax: (+86) 10-6275-1708
E-mail: JBhuang@pku.edu.cn

Supporting information for this article is available on the WWW under http://dx.doi.org/10.1002/chem.201003255.

dine attached to either end of a polyether chain, mixed with Eu^{III}.

Inspired by our previous research on metal–cholate supramolecular self-assembly,[9] we are interested in the rational design of functional lanthanide-containing hybrid hydrogels fabricated by means of bottom-up self-assembly. In this work, organic–inorganic hydrogels based on a europium–cholate system are systematically investigated, and demonstrated as red-light emitters. The self-assembled hydrogel, which has good mechanical intensity, is found to be composed of 1D nanofibers and helical nanofibers. The increase in the photoluminescence of the lanthanide ions is realized by co-assembly with sodium cholate. The photoluminescence emission of hybrid hydrogels with varied europium/cholate molar ratios is investigated to study the effect of stoichiometry on luminescence emission. A possible scheme is presented to relate the photoluminescence intensity with the molecular self-assembly at nanoscale. It is further proven to be a general route to fabricate luminescent hydrogels from cholate and different Ln^{3+} (Ln = Tb, Tb/Eu). Finally, the luminescent Ln^{3+}–cholate hybrid hydrogels can be exploited to synthesize luminescent inorganic nanotubes through a self-templating approach, in which lanthanide ions can serve as both the inorganic precursor and a constituent of the template.[9a] To the best of our knowledge, this is the first time that a series of lanthanide oxysulfide nanotubes with high photoluminescent performance are synthesized in aqueous solution. It is anticipated that these 1D nanomaterials, such as nanotubes, may have significant commercial applications, for example, in radiation intensifying screens, X-ray-computed tomography, oxygen storage, and medical imaging radiation detectors.[10]

Results and Discussion

Photoluminescence emission of Eu^{3+}–cholate hybrid: Sodium cholate (shown here) is a facial amphiphile, which can self-organize into small micelles in water. In the presence of metal ions, supramolecular hydrogels can be obtained in metal-ion–cholate systems. In this work, Eu^{3+} is introduced into a sodium cholate solution to generate functional photoluminescent hydrogels in a convenient way. As shown in the inset of Figure 1a, the Eu^{3+}–cholate system self-assembles into hybrid hydrogel at room temperature; the gel is a red-light emitter under UV light irradiation (≈365 nm). Figure 1a gives the excitation and emission luminescent spectra of the Eu^{3+}–cholate hybrid hydrogel (1.0/3.0 mM). The excitation spectrum monitored within the $^5D_0 \rightarrow {}^7F_2$ transition ($\lambda_{em} = 618$ nm) is composed by a series of intra-4f^6 lines ascribed to transitions between the $^7F_{0,1}$ levels and the $^5L_6$, $^5D_{1-4}$, and $^5G_{2-4}$ excited states. The emission spectrum consists of a series of lines ascribed to the intra-4f^6 $^5D_0 \rightarrow {}^7F_{0-4}$ transitions under direct intra-4f^6 excitation ($\lambda_{ex} = 395$ nm). It should be mentioned that the photoluminescence emission of Eu^{3+} is greatly enhanced in the presence of cholate without notable change in the luminescent spectra. This means the enhancement of the photoluminescence performance of europium ions is realized by their coupling with cholates. The presence of only one peak for $^5D_0 \rightarrow {}^7F_0$ indicates that the Eu^{3+} ion occupies only a single site and a single chemical environment exists around it.[11] The more intense emission of $^5D_0 \rightarrow {}^7F_2$ than those other transitions suggests the Eu^{3+}–cholate hybrid has a good color purity. The decay curve of $^5D_0$ emission is monitored within the $^5D_0 \rightarrow {}^7F_2$ emission line under direct intra-4f^6 excitation (Figure 1b). The curve displays a single exponential behavior, indicating the presence of a single type of local environment for Eu^{3+}[11], which is consistent with the single peak for $^5D_0 \rightarrow {}^7F_0$. The lifetime value ($\tau$) and quantum efficiency are calculated to be about 948 μs and 25.1%. Interestingly, the lifetime of our hybrid hydrogel is relatively long compared to most reported values of 200–600 μs in the literature.[8a]

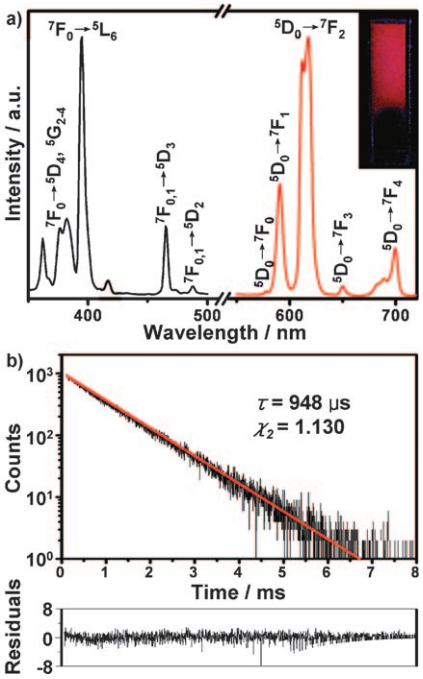

Figure 1. Eu^{3+}–cholate luminescent hydrogels (1.0/3.0 mM). a) Room-temperature excitation spectrum ($\lambda_{em} = 618$ nm) and emission spectrum ($\lambda_{ex} = 395$ nm). The inset shows visual photo of hydrogel in an inverted test tube under 365 nm illumination (concentration of Eu^{3+}–cholate was 10/30 mM). b) Emission decay curve.

Influence of europium/cholate molar ratio on photoluminescent property: The sodium cholate concentration was varied to investigate the effect of europium/cholate molar ratio on

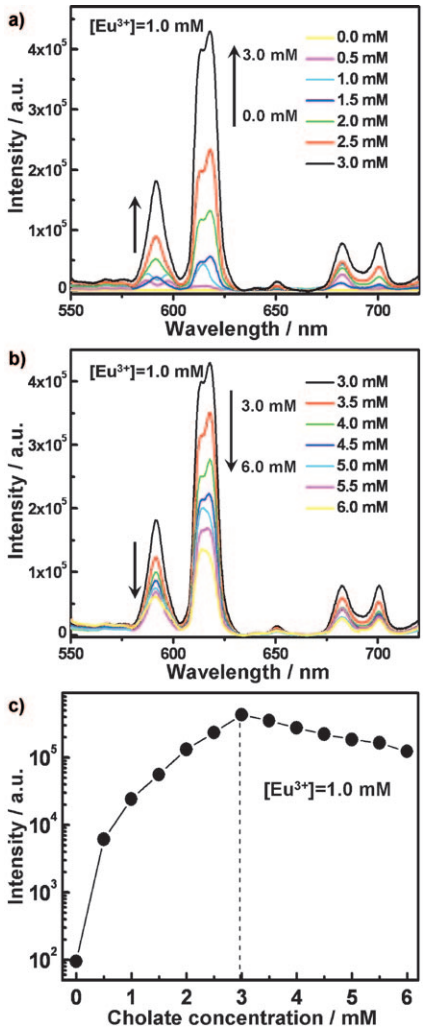

Figure 2. Emission spectra of 1.0 mM Eu^{3+} with varied cholate concentrations: a) 0.0–3.0 mM and b) 3.0–6.0 mM. c) Emission intensity of the $^5D_0 \rightarrow {}^7F_2$ transition peak as a function of sodium cholate concentration.

the photoluminescent performance of europium ion. As shown in Figure 2a, the luminescent emission of europium ions is quite weak in aqueous solution in the absence of sodium cholate. However, upon addition of sodium cholate the luminescence emission of Eu^{3+} increases rapidly. The maximum luminescence emission intensity in a europium–cholate system is found for 1.0/3.0 mM, which is three orders of magnitude higher than that of an aqueous solution of $Eu(NO_3)_3$ (Figure 2c). Nevertheless, continuous addition of sodium cholate results in a slight decrease of luminescent emission at higher cholate concentrations (Figure 2b). This phenomenon is interesting, and will be discussed further below. Furthermore, at low cholate concentrations, such as 0.5 or 1.0 mM, the Eu^{3+} $^5D_0 \rightarrow {}^7F_0$ emission splits into two peaks. This may be interpreted as the existence of two different Eu^{3+} environments in these systems. When the cholate concentration increases, the split can no longer be seen.

Hydrogelation ability and rheological property: The hydrogelation ability and mechanical intensity of the Eu^{3+}–cholate system was further investigated. It is interesting that a self-assembled hydrogel can be obtained at extremely low concentration, ≈0.3 mM europium nitrate and 0.9 mM sodium cholate, and means that one Eu^{3+}–cholate complex traps around 185000 water molecules. This hydrogel belongs in the scope of super hydrogels.[12] The nondestructive frequency sweep in Figure 3a demonstrates that the Eu^{3+}–cholate

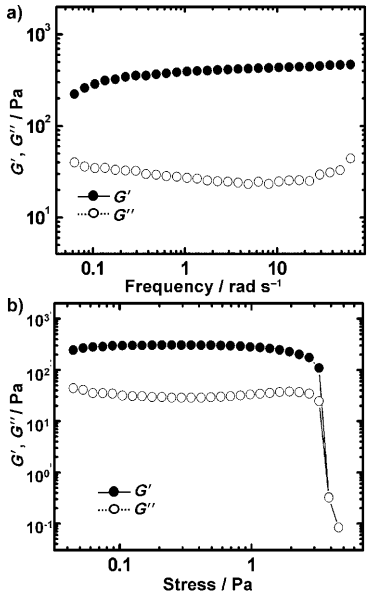

Figure 3. Dynamic rheology of Eu^{3+}–cholate luminescent hydrogels (1.0/3.0 mM). a) Frequency sweep. b) Dynamic stress sweep. The solid symbols are donated to storage modulus G', and the open symbols to loss storage G".

hydrogel (1.0/3.0 mM) exhibits typical solidlike rheological behavior with the storage modulus G' (≈400 Pa) dominating the loss modulus G'' (≈25 Pa) over the investigated oscillating frequency. Additionally, the amplitude sweep (f= 1 Hz) in Figure 3b indicates weak dependence of G' and G'' on applied stress until the yield stress (≈3 Pa) is reached. When the gelator concentration is increased, the hydrogel mechanical intensity can be greatly enhanced. For example, the storage modulus G' and the loss modulus G'' increase to 3000 and 200 Pa, respectively, as the concentration increases to 2.0/6.0 mM in the Eu^{3+}–cholate system. Meanwhile, the yield stress of this system is also improved to 15 Pa (Figure S1 in the Supporting Information).

Supramolecular nanostructures in Eu^{3+}–cholate hybrid: Fluorescence microscopy and TEM are performed to reveal the self-assembled nanostructures in Eu^{3+}–cholate hydrogels. The incorporation of europium ions can impart self-indicative advantages to supramolecular nanofibers, in which europium serves as the indicative agent under fluorescence microscopy. By utilizing a filtered 365 nm UV laser, a large amount of 1D, flexible fibrous structure showing a bright

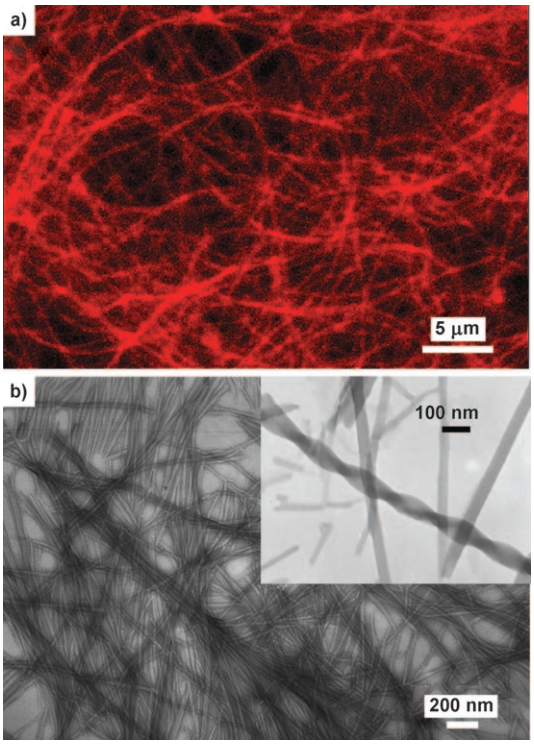

Figure 4. Morphology of Eu^{3+}–cholate hybrids (1.0/3.0 mM). a) Fluorescence microscopic image with 365 nm UV light excitation. b) TEM image of nanofibers and the inset show helical nanofibers.

red emission (the characteristic emission color of Eu^{3+} ions) is observed in the Eu^{3+}–cholate hybrid hydrogel (1.0/3.0 mM). The fibers extend to tens of micrometers in length and entangle with each other to form a 3D network (Figure 4a). TEM without staining regents was also performed to get a clearer picture of the microstructures. As shown in Figure 4b, the self-assembled nanofibers are 10–50 nm in width and several μm in length. Helical nanofibers can also be observed in the TEM images (Figure 4b inset). It should be noted that photoluminescent 1D nanostructures containing lanthanide ions are rarely reported.[13]

Combined with the above results, the strong photoluminescence emission, long luminescence decay life, and Eu^{3+}–cholate stoichiometry in hybrid hydrogels is discussed and a possible illustration is proposed in Scheme 1. The photoluminescence enhancement and long luminescence decay life is suggested to originate from Eu^{3+}–cholate coordination and self-assembly. This is because the water hydroxyl groups can quench the luminescence of lanthanide ions (hydroxyl quenching). The high-energy vibrations associated with the hydroxyl groups can couple with the excited electronic states of the lanthanide ions, and this provides an efficient channel for deactivation of the excited states through nonradiative relaxation.[14] Upon the addition of sodium cholate, the Eu^{3+} nonradiative relaxation of the excited states by water hydroxyl groups can be suppressed through the coordination of Eu^{3+} by a carboxyl group. Particularly, the co-assembly of Eu^{3+} with cholate embeds Eu^{3+} inside the nanofibers, thus, shielding it from water quenching. Therefore, the Eu^{3+} luminescence emission is greatly enhanced (Figure 2a).

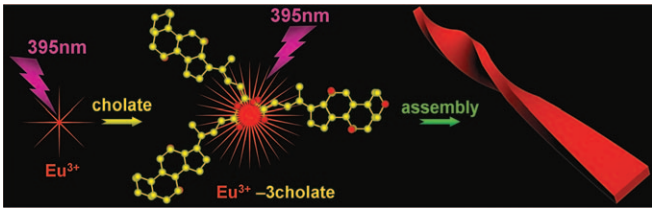

Scheme 1. Schematic model of Eu^{3+}–cholate luminescent nanoribbon formation.

As stated above, when the concentration of sodium cholate is relatively low (0.5 or 1.0 mM), the $^5D_0 \rightarrow {}^7F_0$ emission split into two peaks (Figure 2a). This can be interpreted as the Eu^{3+} ions occupying two types of chemical environments.[11] In this system, some Eu^{3+} ions coordinate with cholate and are embedded inside the nanofibers; while others are in a free state without coordination to cholate. Upon further addition of sodium cholate, most of the Eu^{3+} ions incorporate into nanofibers and consequently the split disappears.

Although the addition of sodium cholate greatly enhances the Eu^{3+} photoluminescence emission, continuous addition of sodium cholate (>3.0 mM) results in a slight decrease of luminescence intensity. This can be rationalized in that Eu^{3+} and cholate co-assemble into nanofibers with 1:3 stoichiometry. In other words, one Eu^{3+} ion coordinates with three cholate molecules, which can be confirmed by electrospray ionization mass spectra (ESI-MS, Figure S2 in the Supporting Information). When the sodium cholate concentration exceeds 3.0 mM, cholate is in excess. It is well acknowledged that sodium cholate is a solubilization agent and, hence, excessive sodium cholate may disassemble the supramolecular fibers in Eu^{3+}–cholate systems.[15] Therefore, the embedment of Eu^{3+} into nanofibers is weakened and luminescent emission will be lowered. In our experiment, addition of excessive sodium cholate destroyed Eu^{3+}–cholate hydrogels, which supports our explanation.

Photoluminescent Ln^{3+}–cholate hybrid with tunable emission colors: Different kinds of photoluminescent hybrid hydrogels with tunable emission colors can be obtained from sodium cholate and different lanthanide ions. Figure 5a gives convincing evidence of photoluminescent spectra of Tb^{3+}–cholate hydrogel. The spectrum exhibits typical character of lanthanide ions in aqueous solution. The Tb^{3+}–cholate hybrid hydrogel shows green-light emission under UV light excitation at room temperature (Figure 5a inset). The emission spectrum displays a series of straight lines ascribed to the intra-$^4f_8$ $^5D_4 \rightarrow {}^7F_{6-0}$ transitions. The $^5D_4$ lifetime emission decay curve displays a single-exponential mode with the lifetime value of 1142 μs (Figure S3a in the Supporting Information). Moreover, the photoluminescence color of Ln^{3+}–cholate hydrogel can be also adjusted by doping other

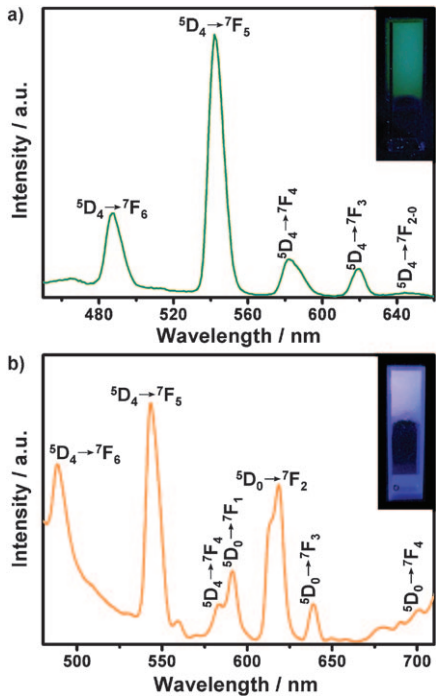

Figure 5. Emission spectrum of photoluminescent hydrogels (1.0/3.0 mM) at room temperature. a) Tb^{3+}–cholate ($\lambda_{ex}=370$ nm). b) Co-doped Tb^{3+}/Eu^{3+} hybrids ($Tb^{3+}/Eu^{3+}=99{:}1$, $\lambda_{ex}=370$ nm). The insets show the luminescent hydrogels in inverted test tubes with the excitation wavelength of 365 nm. (The concentration of Ln^{3+}–cholate is 10/30 mM.)

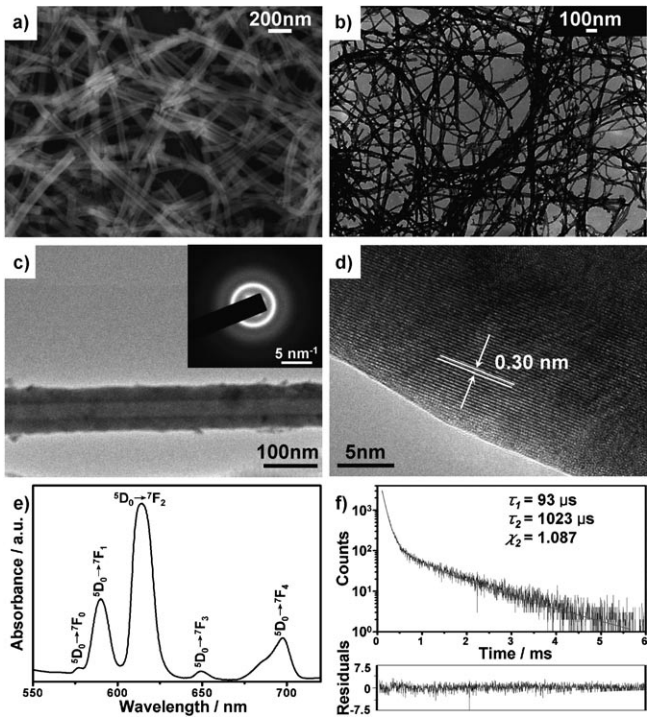

Figure 6. a) FE-SEM and b) TEM images of Eu_2O_2S nanotubes. c) High-magnification TEM and ED pattern (inset). d) HRTEM image. e) Room-temperature emission spectrum ($\lambda_{ex}=395$ nm) of Eu_2O_2S nanotube. f) Photoluminescence decay curve.

lanthanide ions. As shown in inset of Figure 5b, the photoluminescent hydrogel with bisque color emission can be designed in Tb^{3+}/Eu^{3+}–cholate system ($Tb^{3+}/Eu^{3+}=99{:}1$). The characteristic emissions from Tb^{3+} and Eu^{3+} are detected in the photoluminescent spectrum, which is excited by 370 nm light. It is further anticipated that luminescent hydrogels with varying colors are available by changing the Tb^{3+}/Eu^{3+} ratio or co-doping different lanthanide ions. It is interesting to note that the photoluminescent property can be further adjusted by changing the excitation wavelength. For example, in the Tb^{3+}/Eu^{3+}–cholate hydrogel ($Tb^{3+}/Eu^{3+}=99{:}1$), the Tb^{3+} emission is suppressed under 395 nm excitation (Figure S3b in the Supporting Information) and a pink hybrid hydrogel are obtained.

Preparation of Eu_2O_2S nanotubes based on the Eu^{3+}–cholate supramolecular system: It is worth noting that lanthanide oxysulfide nanotubes, which are rarely prepared through a solution route,[16] are conveniently obtained by means of a self-templating approach in the Ln^{3+}–cholate hybrid hydrogel. In this strategy, metal ions serve as both the inorganic precursor and a constituent of the soft template, which is further deposited from supramolecular self-assemblies to generate inorganic nanomaterials with corresponding shape. For example, europium oxysulfide nanotubes are prepared by adding Na_2S solution to Eu^{3+}–cholate hydrogels in the absence of protective conditions. Field emission scanning electron microscopy (FE-SEM, Figure 6a) and TEM (Figure 6b) provide large-scale views of massive uniform high-axial-ratio Eu_2O_2S nanotubes. The diameters of the nanotubes are in the range of 50–80 nm. The enlarged TEM image in Figure 6–c clearly exhibits a typical nanotube. The electron diffraction (ED) pattern (inset of Figure 6–c) illustrates the nanotube is polycrystalline in nature. A high-resolution TEM image (HRTEM, Figure 6d) indicates that the tubes are well-crystallized and have an interplanar spacing of 0.30 nm, corresponding to the (011) planes of hexagonal Eu_2O_2S. The energy-dispersive spectroscopy (EDS, Figure S4a in the Supporting Information) results also prove the formation of Eu_2O_2S nanotubes. X-ray diffraction (XRD, Figure S4b in the Supporting Information) can be indexed with space group $P\bar{3}m1$ (JCPDS no. 26-1418). It is noted that the size and morphology of Eu_2O_2S tubes are in good agreement with Eu^{3+}–cholate nanofibers, which indicate the successful transcription of the soft template into Eu_2O_2S nanotubes. The emission spectrum of Eu_2O_2S nanotubes consists of a series of lines which ascribe to the intra-$4f^6$ $^5D_0 \rightarrow {}^7F_{0-4}$ transitions (Figure 6e). The emission spectrum is broadened, and the ratio of the emission intensity at 614 nm to that at 623 nm is evidently enhanced compared with that of the bulk sample.[15d] The $^5D_0$ emission decay curve of Eu_2O_2S (Figure 6f) was monitored within the $^5D_0 \rightarrow {}^7F_2$ emission line under direct intra-$4f^6$ excitation ($^5L_6$, 395 nm). The curve displays a double exponential behavior, indicating the presence of two types of Eu^{3+} local environment, that is, on the surface and in the in-

terior of nanotubes, yielding the lifetime value (τ) of 93 and 1023 μs and a quantum efficiency of 2%. The quantum efficiency value is lower than that of bulk lanthanide oxysulfide phosphors, probably because of the drastically enlarged surface-to-volume ratio favoring recombination, which does not engender visible emission.[16]

Preparation of Eu^{3+}-doped lanthanide oxysulfide nanotubes: A series of luminescent Eu^{3+}-doped lanthanide oxysulfide nanotubes, such as Eu^{3+}-doped Gd_2O_2S and Y_2O_2S, can be prepared by means of a self-templating approach in Gd^{3+}–cholate:Eu^{3+} (5%) and Y^{3+}–cholate:Eu^{3+} (5%) hybrid hydrogels. The Eu^{3+}-doped Gd^{3+}– and Y^{3+}–cholate hybrids are also composed of 1D fibrous structures (Figure 7a and c), which can be used as a soft template to synthesize lanthanide oxysulfide nanotubes. As indicated in TEM images (Figure 7b and d), Gd_2O_2S:Eu and Y_2O_2S:Eu nanotubes are achieved in high yield and good uniformity by following the preparative method given in Experimental Section. EDS (Figure S5c and S6c in the Supporting Information) and powder XRD (Figure S5d and S6d in the Supporting Information) have demonstrated the successful synthesis of $P\bar{3}m1$ space group Gd_2O_2S and Y_2O_2S. ED patterns (Figure S5a and S6a inset in the Supporting Information) indicate the nanotubes are polycrystalline. HR-TEM images reveal highly crystallized tubes and gives typical interplanar spacing (Figure S5b and S6bin the Supporting Information). Gd_2O_2S:Eu and Y_2O_2S:Eu nanotubes also show luminescent properties similar to those of Eu_2O_2S nanotubes, though they exhibit a stronger emission intensity (Figure S5e and S6e in the Supporting Information) and longer life time (Figure S5f and S5f in the Supporting Information). Therefore, this method is expected to be a simple and convenient route to create 1D lanthanide oxysulfide nanotubes. Moreover, it can be rationally envisioned that multiple compositional or doped nanotubes may be constructed when a multi-metal-ion assembly and/or a multi-reactant-agent is employed in this synthetic strategy.

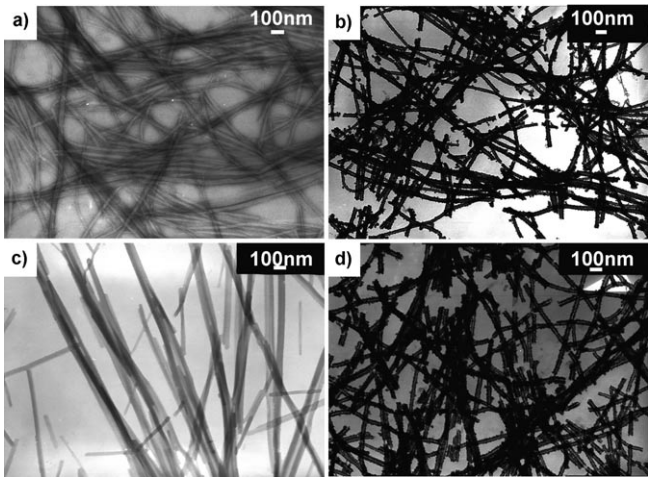

Figure 7. TEM images of self-assembled nanofibers in a) Y^{3+}/Eu^{3+}–cholate ($Y^{3+}/Eu^{3+}=95/5$) hybrid hydrogel and c) Y^{3+}/Eu^{3+}–cholate ($Y^{3+}/Eu^{3+}=95:5$) hybrid hydrogel. TEM images of lanthanide oxysulfide nanotubes prepared by self-templating strategy of b) Gd_2O_2S:Eu nanotubes and d) Y_2O_2S:Eu nanotubes.

Conclusion

In conclusion, photoluminescent lanthanide–cholate hybrid hydrogels are conveniently fabricated through bottom-up self-assembly. In a typical case, Eu^{3+}–cholate hybrids that are room temperature red-light emitters with long lifetime were systematically investigated. The luminescence enhancement in supramolecular hydrogel was realized by means of Eu^{3+}–cholate coordination and nanofiber formation. It was found that the photoluminescence emission intensity of the hydrogel exhibits a strong dependence on the europium/cholate molar ratio, with the maximum emission appearing at a stoichiometry of 1:3. Moreover, the emission color of a lanthanide–cholate hydrogel can be tuned by utilizing different lanthanide ions or co-doping ions. Finally the metal-containing hybrids were exploited to synthesize oxysulfide nanotubes, in which metal ions serve as both inorganic precursor and a constituent of the template. This is the first time that photoluminescent lanthanide oxysulfide nanotubes were obtained by using mild conditions. Thus, we anticipate that lanthanide–cholate hybrids are appealing soft matter materials that may find further application in the fields of biotechnology, optoelectronic devices, and sensors.

Experimental Section

Materials: Sodium cholate (Alfa Aesar, 99%), metal nitrates and other chemicals (A.R. Grade of Beijing Chemical Co.) were used as received.

Preparation of lanthanide–cholate hybrid hydrogels: The lanthanide–cholate hybrid hydrogels were obtained by directly vortex mixing sodium cholate solution with the desired amount of a concentrated lanthanide nitrates solution (0.1 or 0.5 M). Typically, sodium cholate solution (2 mL, 3 mM) was incubated at 25 °C for at least 1 h. Then it was vortexed while $Eu(NO_3)_3$ (20 mL, 0.1 mM) was added. The resulting mixture was maintained at 25 °C in a thermostated bath at least for three days before further analyses. During this period, a self-supporting hydrogel formed.

Preparation of lanthanide oxysulfide nanotubes: In a typical synthesis, lanthanide–cholate hybrid hydrogels (2 mL, 1.0/3.0 mM for europium–cholate, 5% europium-doped gadolinium–cholate, and 5% europium-doped yttrium–cholate) was added to an aqueous solution of Na_2S (2 N, 100 mM) in the absence of protective conditions. Agitation was not needed. The deposition reactions progressed at the interface of the hydrogel and the Na_2S solution. After the reaction was complete, the hydrogel was destroyed and the precipitation at the bottom of the test tube was collected by centrifugation and washed several times with deionized water.

Characterization of lanthanide–cholate hybrid hydrogels: The steady-state photoluminescent spectra were measured with an Edinburgh Instruments FLS920 spectrofluorometer by using a monochromated Xe lamp as an excitation source. Time-resolved fluorescence spectra measurements were performed with a Lifespec Red spectrofluorometer from Edinburgh Instruments equipped with a Hamamatsu picosecond light pulsar

C8898 using a 393 nm laser with a repetition rate of 1 MHz as light source. For each measurement, at least 3000 photon counts were collected in the peak channel to ensure the decay quality. The goodness-of-fit of decay curves, χ^2, was no more than 1.3. The quantum efficiency was calculated as described in reference [17]. Photographs were taken with a Sony CyberShot DSC-T100 digital camera under a filtered 365 nm UV lamp.

The rheological properties of lanthanide–cholate hybrid hydrogels were measured at 25 ± 0.05 °C with a Thermo Haake RS300 rheometer (cone and plate geometry of 35 mm in diameter with the cone gap equal to 0.105 mm). A solvent trap was used to avoid water evaporation. Frequency spectra were conducted in the linear viscoelastic regime of the samples determined from dynamic strain sweep measurements.

For fluorescence microscopy observations, a slice of hydrogel was placed onto a pre-cleaned glass surface, and was subsequently covered with a slide. The edge of the slide was sealed with 3–4 successive coats of clear nail polish to avoid evaporation. The microstructure observation was conducted on a Leica Tcs-sp confocal laser-scanning microscope under a filtered 365 nm UV laser.

For TEM, a slice of hydrogel was placed on copper grid and then dried freely under ambient conditions and desired temperature. The hydrogels were characterized by transmission electron microscopy (TEM, JEM-100CX, 100 kV).

ESI-MS measurements were performed on a Bruker Apex IV Fourier Transform Ion Cyclotron Resonance (FT-ICR) mass spectrometer in positive mode. Electrospray ionization mass spectra (ESI-MS) conditions were optimized to favor the observation of noncovalent complexes.

Characterization of lanthanide oxysulfide nanotubes: The obtained nanotubes were characterized by SEM (Hitachi S4800, 10 kV), TEM (JEOL JEM-100CX, 100 kV), HRTEM (FEI Tecnai F30, 300 kV), XRD (Rigaku Dmax-2000, Ni-filtered $Cu_{K\alpha}$ radiation). For the TEM and SEM measurements, the obtained products were dispersed in water and dropped onto a Formvar-covered copper grid and a silicon wafer, respectively, followed by drying naturally. For XRD measurements, several drops of the suspension were dropped on a clean glass slide, followed by drying in air. Photoluminescent measurements were performed on an Edinburgh Instruments FLS920 lifetime and steady-state fluorescence spectrophotometer.

Acknowledgements

This work was supported by National Natural Science Foundation of China (20873001, 20633010, 50821061, and 21073006) and National Basic Research Program of China (Grant No. 2007CB936201). We would like to thank Prof. Lingdong Sun for helpful discussions and suggestions.

[1] a) K. Binnemans, *Chem. Rev.* **2009**, *109*, 4283; b) M. Bottrill, L. Kwok, N. J. Long, *Chem. Soc. Rev.* **2006**, *35*, 557; c) C. M. G. dos Santos, A. J. Harte, S. J. Quinn, T. Gunnlaugsson, *Coord. Chem. Rev.* **2008**, *252*, 2512; d) J. H. Yu, D. Parker, R. Pal, R. A. Poole, M. J. Cann, *J. Am. Chem. Soc.* **2006**, *128*, 2294; e) G. S. Shao, R. C. Han, Y. Ma, M. X. Tang, F. X. Xue, Y. L. Sha, Y. Wang, *Chem. Eur. J.* **2010**, *16*, 8647; f) C. H. Song, Z. Q. Ye, G. L. Wang, J. L. Yuan, Y. F. Guan, *Chem. Eur. J.* **2010**, *16*, 6464; g) E. Deiters, B. Song, A.-S. Chauvin, C. D. B. Vandevyver, F. Gumy, J.-C. G. Bünzli, *Chem. Eur. J.* **2009**, *15*, 885.

[2] a) J.-C. G. Bünzli, C. Piguet, *Chem. Soc. Rev.* **2005**, *34*, 1048; b) J.-C. G. Bünzli, *Acc. Chem. Res.* **2006**, *39*, 53.

[3] a) G. F. de Sá, O. L. Malta, C. de Mello Donegá, A. M. Simas, R. L. Longo, P. A. Santa-Cruz, E. F. da Silva Jr, *Coord. Chem. Rev.* **2000**, *196*, 165; b) Y. Hasegawa, Y. Wada, S. Yanagida, *J. Photochem. Photobiol. C* **2004**, *5*, 183; c) L. R. Melby, N. J. Rose, E. Abramson, J. C. Caris, *J. Am. Chem. Soc.* **1964**, *86*, 5117; d) E. S. Andreiadis, R. Demadrille, D. Imbert, J. Pécaut, M. Mazzanti, *Chem. Eur. J.* **2009**, *15*, 9458; e) F. Stomeo, C. Lincheneau, J. P. Leonard, J. E. O'Brien, R. D. Peacock, C. P. McCoy, T. Gunnlaugsson, *J. Am. Chem. Soc.* **2009**, *131*, 9636.

[4] a) K. Binnemans, C. Görller-Walrand, *Chem. Rev.* **2002**, *102*, 2303; b) N. M. Shavaleev, S. V. Eliseeva, R. Scopelliti, J.-C. G. Bünzli, *Chem. Eur. J.* **2009**, *15*, 10790; c) R. Nishiyabu, N. Hashimoto, T. Cho, K. Watanabe, T. Yasunaga, A. Endo, K. Kaneko, T. Niidome, M. Murata, C. Adachi, Y. Katayama, M. Hashizume, N. Kimizuka, *J. Am. Chem. Soc.* **2009**, *131*, 2151; d) E. Terazzi, L. Guénée, B. Bocquet, J.-F. Lemonnier, N. D. Favera, D. Piguet, *Chem. Eur. J.* **2009**, *15*, 12719; e) K. Liu, H. P. You, Y. H. Zheng, G. Jia, Y. H. Song, Y. J. Huang, M. Yang, J. J. Jia, N. Guo, H. J. Zhang, *J. Mater. Chem.* **2010**, *20*, 3272; f) C. Wang, R. J. Zhang, H. Möhwald, *Langmuir* **2010**, *26*, 11987; g) L. D. Carlos, R. A. S. Ferreira, V. de Zea Bermudez, S. J. L. Ribeiro, *Adv. Mater.* **2009**, *21*, 509; h) C. Aimé, R. Nishiyabu, R. Gondo, N. Kimizuka, *Chem. Eur. J.* **2010**, *16*, 3604.

[5] a) *Molecular Gels: Materials with Self Assembled Fibrillar Network* (Eds.: R. G. Weiss, P. Terech), Spinger, Dordrecht, **2006**; b) L. A. Estroff, A. D. Hamilton, *Chem. Rev.* **2004**, *104*, 1201; c) N. M. Sangeetha, U. Maitra, *Chem. Soc. Rev.* **2005**, *34*, 821; d) M. de Loos, B. L. Feringa, J. H. van Esch, *Eur. J. Org. Chem.* **2005**, 3615; e) K. Trickett, J. Eastoe, *Adv. Colloid Interface Sci.* **2008**, *144*, 66.

[6] a) A. P. Esser-Kahn, A. T. Iavarone, M. B. Francis, *J. Am. Chem. Soc.* **2008**, *130*, 15820; b) S. Kiyonaka, K. Sada, I. Yoshimura, S. Shinkai, N. Katoand, I. Hamachi, *Nat. Mater.* **2003**, *3*, 58; c) J. D. Hartgerink, E. Beniash, S. I. Stupp, *Science* **2001**, *294*, 1684; d) F. Zhao, M. L. Ma, B. Xu, *Chem. Soc. Rev.* **2009**, *38*, 883; e) A. Friggeri, B. L. Feringa, J. van Esch, *J. Controlled Release* **2004**, *97*, 241; f) R. G. Ellis-Behnke, Y. X. Liang, S. W. You, D. K. C. Tay, S. G. Zhang, K. F. So, G. E. Schneider, *Proc. Natl. Acad. Sci. USA* **2006**, *103*, 5054; g) K. Y. Lee, D. J. Mooney, *Chem. Rev.* **2001**, *101*, 1869; h) K. J. C. van Bommel, A. Friggeri, S. Shinkai, *Angew. Chem.* **2003**, *115*, 1010; *Angew. Chem. Int. Ed.* **2003**, *42*, 980; i) J. H. Jung, S.-H. Lee, J. S. Yoo, K. Yoshida, T. Shimizu, S. Shinkai, *Chem. Eur. J.* **2003**, *9*, 5307.

[7] a) C. P. McCoy, F. Stomeo, S. E. Plush, T. Gunnlaugsson, *Chem. Mater.* **2006**, *18*, 4336; b) V. A. Smirnov, G. A. Sukhadolski, O. E. Philippova, A. R. Khokhlov, *J. Phys. Chem. B* **1999**, *103*, 7621; c) Q. Wang, K. Ogawa, K. Toma, H. Tamiaka, *Chem. Lett.* **2008**, *37*, 430.

[8] a) F. Liu, L. D. Carlos, R. A. S. Ferreira, J. Rocha, M. C. Gaudino, M. Robitzer, F. Quignard, *Biomacromolecules* **2008**, *9*, 1945; b) H. Wang, X. Li, F. Fang, Y. J. Yang, *Dalton Trans.* **2010**, *39*, 7294; c) V. A. Smirnov, O. E. Philippova, G. A. Sukhadolski, A. R. Khokhlov, *Macromolecules* **1998**, *31*, 1162; d) G. De Paoli, Z. Džolic, F. Rizzo, L. De Cola, F. Vögtle, W. M. Müller, G. Richardt, M. Žinic, *Adv. Funct. Mater.* **2007**, *17*, 821; e) S. J. Rowan, J. B. Beck, *Faraday Discuss.* **2005**, *128*, 43; f) L. Sambri, F. Cucinotta, G. De Paoli, S. Stagnic, L. De Cola, *New J. Chem.* **2010**, *34*, 2093.

[9] a) Y. Qiao, Y. Y. Lin, Y. J. Wang, Z. Y. Yang, J. Liu, J. Zhou, Y. Yan, J. B. Huang, *Nano Lett.* **2009**, *9*, 4500; b) Y. Qiao, Y. Y. Lin, Z. Y. Yang, H. F. Chen, S. F. Zhang, Y. Yan, J. B. Huang, *J. Phys. Chem. B* **2010**, *114*, 11725; c) Y. Qiao, Y. J. Wang, Z. Y. Yang, Y. Y. Lin, J. B. Huang, *Chem. Mater* **2011**, *23*, 1182.

[10] a) M. Machida, K. Kawamura, K. Ito, K. Ikeue, *Chem. Mater.* **2005**, *17*, 1487; b) M. Machida, K. Kawamura, K. Ito, *Chem. Commun.* **2004**, 662; c) H. Toki, S. Ito, Jpn. Kokai Tokkyo Koho, JP 08 64, 147, **1996**; d) D. Cavouras, I. Kandarakis, T. Maris, G. S. Panayiotakis, C. D. Nomicos, *Eur. J. Radiol.* **2000**, *35*, 70.

[11] H. F. Brito, O. L. Malta, L. R. Souza, J. F. S. Menezes, C. A. A. Carvalho, *J. Non-Cryst. Solids* **1999**, *247*, 129.

[12] a) F. M. Menger, K. L. Caran, *J. Am. Chem. Soc.* **2000**, *122*, 11679; b) H. Kobayashi, A. Friggeri, K. Koumoto, M. Amaike, S. Shinkai, D. N. Reinhoudt, *Org. Lett.* **2002**, *4*, 1423; c) J. Nagasawa, M. Kudo, S. Hayashi, N. Tamaoki, *Langmuir* **2004**, *20*, 7907; d) T. Tu, W. Assenmacher, H. Peterlik, R. Weisbarth, M. Nieger, K. H. Dotz, *Angew. Chem.* **2007**, *119*, 6486; *Angew. Chem. Int. Ed.* **2007**, *46*, 6368; e) J. Liu, P. L. He, J. L. Yan, X. H. Fang, Peng, J. X. , K. Q. Liu, Y. Fang, *Adv. Mater.* **2008**, *20*, 2508.

[13] J. Ryu, S. Y. Lim, C. B. Park, *Adv. Mater.* **2009**, *21*, 1577.

[14] a) N. Sabbatini, M. Guardigli, J.-M. Lehn, *Coord. Chem. Rev.* **1993**, *123*, 201; b) M. Kawa, J. M. J. Fréchet, *Chem. Mater.* **1998**, *10*, 286.
[15] a) S. Nagadome, Y. Okazaki, S. Lee, Y. Sasaki, G. Sugihara, *Langmuir* **2001**, *17*, 4405; b) C. J. O′Connor, R. G. Wallace, *Adv. Colloid Interface Sci.* **1985**, *22*, 1; c) E. Kolehmainen, R. Laatikainen, *J. Colloid Interface Sci.* **1988**, *121*, 148.
[16] a) L. Delgado da Vila, E. B. Stucchi, M. R. Davolos, *J. Mater. Chem.* **1997**, *7*, 2113; b) S. H. Yu, Z. H. Han, J. Yang, H. Q. Zhao, R. Y. Yang, Y. Xie, Y. T. Qian, Y. H. Zhang, *Chem. Mater.* **1999**, *11*, 192; c) O. Kanehisa, T. Kano, H. Yamamoto, *J. Electrochem. Soc.* **1985**, *132*, 2023; d) F. Zhao, M. Yuan, W. Zhang, S. Gao, *J. Am. Chem. Soc.* **2006**, *128*, 11758.
[17] L. D. Carlos, Y. Messaddeq, H. F. Brito, R. A. Sá Ferreira, V. de Zea Bermudez, S. J. L. Ribeiro, *Adv. Mater.* **2000**, *12*, 594.

Received: November 12, 2010
Published online: March 30, 2011

